Numerical Relativity in 3+1 Dimensions

Bernd Brügmann

Max-Planck-Institut für Gravitationsphysik
(Albert-Einstein-Institut)
Am Mühlenberg 1, 14476 Golm, Germany
`bruegman@aei-potsdam.mpg.de`

Abstract

Numerical relativity is finally approaching a state where the evolution of rather general (3+1)-dimensional data sets can be computed in order to solve the Einstein equations. After a general introduction, three topics of current interest are briefly reviewed: binary black hole mergers, the evolution of strong gravitational waves, and shift conditions for neutron star binaries.

1 Introduction

In this short review I describe work concerned with one of the central issues of numerical relativity, the solution of the two body evolution problem of general relativity. After a short introduction to (3+1)-dimensional numerical relativity, I briefly discuss recent progress on binary black hole mergers, the evolution of strong gravitational waves, and shift conditions for neutron star binaries.

As opposed to Newtonian theory, where the Kepler ellipses provide an astrophysically relevant example for the analytic solution of the two body problem, in Einsteinian gravity there are no corresponding exact solutions. The failure of Einstein's theory to lead to stable orbits is due to the fact that in general two orbiting bodies will emit gravitational waves that carry away energy and momentum from the system, leading to an inspiral. But, of course, this "leak" is not considered to be detrimental. Gravitational waves are one of the most interesting new phenomena introduced by general relativity that will open a new window into the universe through gravitational wave astronomy, e.g. [1].

The evolution of a two body gravitational system, for example a binary black hole system (which can be constructed as a vacuum system and avoids additional complication due to matter sources), can be divided into at least three phases. For sufficiently large separation of the two black holes there is a

1

slow inspiral phase with many orbits, followed by a very brief violent merger phase that leads to a single, distorted black hole that after a short ring-down phase settles down to a final stationary black hole. For the initial and final phase rather well understood approximation schemes are available, i.e. post-newtonian calculations for the slow inspiral of two point masses (e.g. [2, 3]) and the close limit approximation for the ring-down of a single distorted black hole(e.g. [4]). For a full treatment of the strongly non-linear, fully general relativistic phase one has to turn to computer simulations to obtain (again approximate) numerical answers.

Each phase leads to a characteristic gravitational wave signal. At this time several gravitational wave detectors are being built world-wide that should for the first time make the direct measurement of gravitational waves possible. The prediction and analysis of future signals is the main motivation for studies of binary systems in numerical relativity. While certainly the primary motivation, let me add that even if it had no direct, in the near future measurable observational consequences, we should solve a basic problem like the two body problem of general relativity.

The article is organized as follows. In Sec. 2, a brief history of black hole evolutions in numerical relativity in 2+1 (axisymmetry) and 3+1 dimensions is given. In Sec. 3, the evolution problem of numerical relativity is introduced in its 3+1 form, leading to three main issues: initial data, evolution, analysis. Initial data is computed on a three-dimensional hypersurface, which is evolved in time, and at various times analysis like identifying the black hole horizons and gravitational wave extraction is carried out. The coordinate problem of numerical relativity is emphasized with the choice of slicing function, the lapse, as an example. The skeleton of a typical black hole evolution is discussed. In Sec. 4, the "Cactus" code, a computational infrastructure for numerical relativity and relativistic astrophysics, is described.

After this general introduction, we discuss several examples for recent progress in (3+1)-dimensional numerical relativity. In Sec. 5, current (summer of 1999) binary black hole simulations are presented. The holes start out close to each other and evolve through a plunge rather than an orbit (a grazing collision). Achievable evolution time is now about $30M$ (M the mass of the final black hole), which for the first time allows the extraction of wave forms. In Sec. 6, a discussion of strong wave evolutions is included because strong waves play a role in black hole mergers and these studies provided the proving ground for a new evolution scheme discussed in Sec. 3.1. In Sec. 7, the minimal distortion shift condition is described. Lapse and shift specify the coordinate gauge, and in all simulations mentioned so far the shift has been zero, but for systems with rotation a shift condition will be essential. The example presented is minimal distortion shift for a binary neutron star system, which for this purpose is simpler than black holes because there are no special inner boundaries.

Sec. 8 concludes this brief review, pointing out again those issues and techniques that will be important for the numerical simulation of binary black holes for several orbits lasting for 100–$1000M$ with results that are relevant for gravitational wave astronomy.

2 History of black hole simulations in numerical relativity

In this section I endeavor to give a necessarily very short but in its highlights complete exposition of the literature on numerical black hole evolutions, concentrating mostly on work that implements the complete black hole evolution problem (data, evolution, analysis) for the full Einstein equations in vacuum. Matter occurs in a few places but only as a means to form black holes. Clearly, there is a large and important body of work concerned with all the different, separate aspects of and methods for black hole evolutions as outlined in Sec. 3. Still, this allows us to sketch the history of the field.

2.1   2+1 dimensions

After some early attempts [5], it was the work by Smarr [6, 7] and Eppley [8] on the head-on collision of two equal mass Misner black holes [9] which basically founded the field of numerical relativity as a subject of computational physics. Axisymmetric head-on collisions allow significant savings in computational cost when formulated with two spatial and one time coordinate (2+1 dimensions), although this excludes the possibility of orbiting black holes and radiation of angular momentum. Many of the key techniques that are still in use today stem from that period of the sixties and seventies (see [10] for the definitive review).

The beginning of the nineties saw a surge of activity when more powerful computers, improved codes and methods allowed significant advances. The axisymmetric collision of black holes, either formed by particles [11] or implemented as Misner data [12, 13], was repeated complete with horizon finding and wave extraction. It is remarkable how the crude results for the wave emission of [6, 7] where confirmed in [12]. Another highlight is certainly the numerical computation of the "pair of pants" picture for a black hole merger [14], which was a result of the US Binary Black Hole Grand Challenge Alliance. Head-on collisions in axisymmetry continue to improve, see the recent work on unequal mass configurations [15, 16].

Another interesting system in axisymmetry are rotating black holes. In [17], particles collapse to form a black hole with rotation and toroidal event horizon. In [18], a Kerr black hole distorted by a gravitational wave is evolved. Matter plus rotating black hole systems are also studied in [19, 20].

A traditional topic in numerical black hole studies is that of black hole formation, of which I want to mention only the following recent references that are of relevance to this article. The formation of naked singularities was examined in [21]. Furthermore, in [22] the collapse of gravitational waves to a black hole is demonstrated. A surprise was that even (1+1)-dimensional, spherically symmetric black hole systems are far from being trivial, as the rich set of critical phenomena discovered by Choptuik [23] showed (see e.g. [24] for a review). In 2+1 dimensions, the only critical collapse studies so far are those of [25].

2.2 3+1 dimensions

Numerical relativity of black holes in 3+1 dimensions was initiated in 1995 with evolutions of a Schwarzschild black hole with singularity avoiding slicing on a Cartesian grid [26]. Achieved run time is about $30M$. At the same time the first (3+1)-dimensional wave simulations were carried out [27, 28]. In Sec. 6, I comment on the collapse of non-axisymmetric waves to a black hole [29].

Returning to our main topic, the evolution of a Schwarzschild black hole with a non-vanishing shift vector was studied in [30], compare Sec. 7. In [31], adaptive mesh refinement techniques, made famous in numerical relativity by [23], were applied for the first time to 3+1 relativity, also for a Schwarzschild black hole. By now, evolutions for the Schwarzschild spacetime are standard code test, e.g. [32]. Further studies of single black holes include the distorted black holes in [33, 34, 35], which provided the first detailed tests of wave extraction in 3+1 dimensions. The Black Hole Grand Challenge Alliance performed the longest, stable evolution of a single black hole so far, reaching about $60M$ for a standard Cauchy evolution with black hole excision and a boosted black hole [36], and essentially achieved complete stability ($> 60000M$) with a characteristic evolution code, which is tailored to the one black hole problem but can also treat small distortions, and for the first time a black hole that moves across the grid [37, 38, 39].

Binary black hole evolutions are pushing the limits of what is currently possible. Some results for the evolution of the axisymmetric Misner data set with the 3+1 code of [26] with singularity avoiding slicing are reported in [40]. The first true (3+1)-dimensional binary black hole evolutions, the grazing collision of nearby spinning and moving black holes, was performed in [41]. This sets the stage for the recent binary black hole simulations of Sec. 5, but first we want to discuss some of the basic issues in numerical relativity.

3 Anatomy of a numerical relativity simulation

3.1 3+1 formulation

The Arnowitt-Deser-Misner (ADM) equations [42, 10] are one of the possibilities to rewrite the Einstein equations as an initial value problem for spatial hypersurfaces. The dynamical fields of the ADM formulation are a 3-metric g_{ab} and its extrinsic curvature K_{ab} on a 3-manifold Σ, both depending on space (points in Σ) and a time parameter, t. The foliation of the 4-dimensional spacetime into hypersurfaces Σ is characterized in the usual way by a lapse function α and a shift vector β^a. The Einstein equations for vacuum become

$$(\partial_t - \mathcal{L}_\beta)\, g_{ab} = -2\alpha K_{ab} \tag{1}$$

$$(\partial_t - \mathcal{L}_\beta)\, K_{ab} = -D_a D_b \alpha + \alpha(R_{ab} - 2K_{ac}K^c{}_b + K_{ab}K) \tag{2}$$

$$0 = D^b(K_{ab} - g_{ab}K) \equiv \mathcal{D}_a, \tag{3}$$

$$0 = R - K_{ab}K^{ab} + K^2 \equiv \mathcal{H}, \tag{4}$$

where R_{ab} is the 3-Ricci tensor, R the Ricci scalar, K the trace of the extrinsic curvature, $\mathcal{L}_\beta$ the Lie derivative for β, and D_a the covariant derivative compatible with the 3-metric. One obtains evolution equations for the metric variables, (1) and (2), and constraint equations that do not contain time derivatives of g_{ab} or K_{ab}, the momentum constraint (3) and the Hamiltonian constraint (4).

These equations are well known, but displaying them explicitly allows me to make a number of basic observations. First of all, these are comparatively simple equations. Even though writing out all the terms in the index contractions, in the definition of R_{ab} and the covariant derivative leads to on the order of 1000 floating point operations per point for a typical finite difference representation of (1) and (2), this can be easily dealt with computationally and is not one of the fundamental problems of black hole evolutions. Still, a numerical implementation requires some thought and hard work, see Sec. 4.

Notice that lapse and shift appear in the evolution equations (as of course they have to) and have to be specified as part of the evolution problem. Choosing lapse and shift fixes the coordinate gauge for the evolutions, and is one of the key problems for numerical evolutions, see Sec. 3.2.

The constraint equations imply that specifying initial data g_{ab} and K_{ab} on a hypersurface Σ involves in general solving the constraints numerically. If the constraints are satisfied initially, they will remain satisfied for a well-posed evolution system, but this is an analytic statement that is only approximately true numerically.

Finally, the ADM equations do not define a hyperbolic evolution system (e.g. [43]), and it is not clear to what extent the original ADM equations can lead to a numerically stable evolution system. The issue of stability has to be addressed on two levels. First, a well-posed evolution system is one for which existence, uniqueness and stability of a solution for at least finite time intervals can be shown, which is true for example for hyperbolic systems. However, in general stability does not rule out exponentially growing modes (this may be the solution one is looking for). Second, the numerical implentation of an analytically stable system does not trivially lead to stable numerical evolutions (e.g. the finite-differenced equations may have exponentially growing solutions which are not present analytically). Also note that important stability issues arise at the boundaries of the computational domain.

Finding stable evolution systems is perhaps the other key issue in numerical relativity besides the choice of coordinate problem. For an excellent review of first order hyperbolic systems for relativity see [44], but other systems are of interest, too. One of the important developments of the last year was the demonstration by Baumgarte and Shapiro [45], that a conformal, trace-split version of the ADM system very much like the system used by Shibata and Nakumara in [27], is significantly more stable (numerically) than the ADM equations for weak fields and some algebraic slicings. This BSSN system can also be understood as a second order, conformal version of the Bona-Massó system [46]. First order hyperbolic versions were given in [47, 48], although the
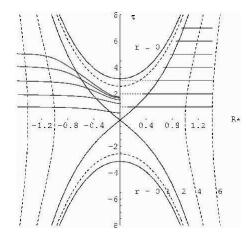
5

Figure 1: Schwarzschild black hole in Novikov coordinates, $M = 1$.

BSSN system as it stands is not hyperbolic. The BSSN variables are

$$
\begin{aligned}
\phi &= \ln(\det g)/12, & (5) \\
K &= g^{ab}K_{ab}, & (6) \\
\tilde{g}_{ab} &= e^{-4\phi}g_{ab}, & (7) \\
\tilde{A}_{ab} &= e^{-4\phi}(K_{ab} - g_{ab}K/3), & (8) \\
\tilde{\Gamma}^c &= \tilde{\Gamma}^c_{ab}\tilde{g}^{ab}, & (9)
\end{aligned}
$$

so that $\det\tilde{g} = 1$ and $\operatorname{tr}\tilde{A}_{ab} = 0$. Furthermore, introducing $\tilde{\Gamma}^c$ leads on the right-hand-side of equation (2) to an elliptic expression in derivatives of $\tilde{g}_{ab}$, i.e. the corresponding BSSN equation has the character of a wave equation. However, including the evolution equation for $\tilde{\Gamma}^c$ appears to spoil hyperbolicity. Nevertheless, the BSSN system has very nice stability properties, and some suggestions about why this may be the case are made in [49]. Several BSSN evolutions have now been reported, for strong waves and maximal slicing [29] (Sec. 6) and also for matter evolutions [50, 51, 52].

3.2 Schwarzschild as an example for a typical black hole evolution problem

Moving on to the prototypical example for a black hole evolution, consider Fig. 1, which shows the Schwarzschild spacetime for a static, spherically symmetric black hole in Novikov coordinates [53, 54]. The coordinates are chosen such that freely falling observers that start at rest at time $\tau = 0$ follow constant R^* lines. The Schwarzschild radius r is related to R^* at $\tau = 0$ through $R^* = (r/(2M) - 1)^{1/2}$. Several constant r lines are shown: the physical singularity at $r = 0$, the event horizon at $r = 2M$, and note how the lines $r = 4M$ and $r = 6M$ curve outwards which corresponds to the radial infall of the observers with constant R^*.

6

To set up an evolution problem we can choose the slice $\tau = 0$ as initial hypersurface with g_{ab} and K_{ab} derived from the Schwarzschild four-metric (g_{ab} and K_{ab} therefore solve the constraints). Note that the physical singularity is to the future of this slice and does not show in g_{ab} and K_{ab}. To perform an evolution, we have to specify lapse and shift. The Novikov coordinates correspond to geodesic slicing, $\alpha = 1$, and vanishing shift, $\beta^a = 0$. Concretely, consider a numerical grid at $\tau = 0$ extending from $R^* = 0$ to $R^* = 2^{1/2}$. In the first quadrant of the figure we have shown how this initial slice moves through the spacetime for geodesic slicing with vanishing shift. Without precaution a numerical code will crash at $\tau = \pi M$ when the point at $R^* = 0$ reaches the singularity (this "crash test" has in fact been used as a first crude code test [26, 31]).

As shown in the figure, one can imagine evolving beyond $\tau = \pi M$ by cutting out from the slice what is inside the event horizon of the black hole, which will not affect the outside of the black hole anyway. "Black hole excision" techniques [55, 56] are a very promising approach to black hole evolutions, although in 3+1 dimensions there remain certain stability problems to be resolved for binary black holes. Black hole excision usually involves a non-trivial choice of lapse and shift.

With black hole excision not quite ready yet, it is so-called singularity avoiding slicings that have been most widely used. Assume $\beta^a = 0$. Primary examples are maximal slicing ($K = 0$ initially and $\Delta\alpha = \alpha K_{ab}K^{ab}$ so that $\partial_t K = 0$), and so-called "1+log" slicings (e.g. $\partial_t \alpha = -\alpha K/2$). In the second quadrant of Fig. 1, we show a typical example (hand-drawn, while the rest of the figure was computed). At the center, evolution slows down, while for large radii the evolution marches on with $\alpha = 1$ at infinity. Obviously, a numerical problem will occur in between, which is referred to as grid-stretching, and which is reflected in growing sharp peaks in the radial-radial component of the metric. Singularity avoiding slicings have this fatal problem built in, but they allow us to compute evolutions up to $30M - 100M$, which is barely sufficient for certain black hole collision and ring-down wave forms.

For completeness let me also mention the possibility of using hyperboloidal slices, or null-slices, or null-slices matched to the spatial slices, which when applicable cover more of the interesting space time in the wave region, e.g. [57, 58, 59, 60, 61, 62, 63, 64]. Characteristic matching is also useful near an excision boundary.

The key point to note is that the choice of coordinates in relativity is a more fundamental problem than, say, the choice of spherical over Cartesian coordinates for computational convenience. There is no simple canonical choice like $\alpha = 1$ and $\beta^a = 0$ that works in reasonably general situations. Even if there are no black holes, geodesic slicing fails due to geodesic focusing. It appears to be the case that one has to determine lapse and shift dynamically during the evolution by some geometric principle as functions of the metric and extrinsic curvature.

7

3.3 Anatomy of a black hole simulation

After discussing 3+1 formulations in general and a specific black hole example, let us list the components of a numerical relativity evolution, with the binary black hole problem as example.

3.3.1 Initial Data

- Choice of hypersurface
  Simplest choice is R^3 for non-black hole data. Black hole data can be, for example, of Misner type with an isometry boundary condition at spheres representing the throats of the holes, $R^3 - spheres$ [65], or Brill-Lindquist type data based on a punctured R^3, $R^3 - points$ [66].

- Solution to constraints
  There are four constraint equations that restrict the choice of 12 components in g_{ab} and K_{ab}. The most common approach is the conformal method [67, 68, 10].

3.3.2 Evolution

- Variables and evolution system
  There are many different choices that can be roughly divided into ADM like systems that are of second order [27, 45], and first order systems that are constructed to obtain hyperbolicity, e.g. [44].

- Choice of coordinates (gauge choice)
  Typically a vanishing shift is used, but see Sec. 7. For the lapse, as explained above, algebraic and elliptic conditions are in use.

- Physical singularities
  Smooth, regular initial data may develop physical singularities which are features of black hole spacetimes. Physical singularities can be avoided by choice of slicing, or removed from the grid through black hole excision.

- Coordinate singularities
  Dynamical determination of lapse and shift may lead to coordinate pathologies, in particular for algebraic slicings (e.g. [69, 70]. Elliptic conditions are sometimes preferable, although they are computationally much more expensive.

- Outer boundary condition
  Asymptotic flatness can be assumed, which implies fall-off conditions for the fields. For run times on the order of $100M$ for a typical singularity avoiding Cauchy evolution, a radiative boundary condition is sufficiently accurate and stable, e.g. [45]. For a more sophisticated scheme see [71]. Also there are two well developed approaches in which the numerical grid does not end at a finite radius but extends to future null infinity, either

by matching to a characteristic code at finite radius [62, 63], or smoothly without matching via a conformal transformation [57, 58, 59, 72]. (Note that in 3+1 dimensions it is no longer straightforward to use a logarithmic radial coordinate as is conventionally done in axisymmetry.)

- Inner boundary conditions
As discussed above, black hole excision leads to a particular inner boundary. As for initial data construction, the inner boundary for slices in a black hole spacetime may be spherical or point-like. For short term evolutions, the numerical slice can cover the inner asymptotically flat regions of the black holes if the resulting coordinate singularities are treated with the puncture method for evolution [26, 41].

3.3.3 Analysis

- Tensor components
The raw output of a computer code will be the components of its basic variables, e.g. g_{ab}, K_{ab}, α, and β^a, all other information is computed from these. Interesting local quantities include Riemann curvature invariants I and J and the Newman-Penrose invariants ψ_0 through ψ_4.

- Black hole horizons
The event horizon of black holes is a spacetime concept and can be found approximately if a sufficiently large spacetime slab has been computed, e.g. [14]. The apparent horizon is a notion intrinsic to the hypersurface (and is therefore slicing dependent). It is defined as the union of outermost marginally trapped surfaces, i.e. surfaces for which the expansion of outgoing null rays vanishes. Trapped surfaces are linked to the existence of black holes through the singularity theorems. See e.g. [73] and references therein for numerical issues.

- Wave extraction
Wave forms can be computed reliably at finite but large radius using the first order gauge invariant approach of [74], as recently demonstrated for 3+1 dimensions in [35]. In approaches that make future null infinity part of the numerical grid, see above, wave extraction is much more direct.

4 Implementation of a numerical relativity simulation

As should be evident from the previous section, numerical relativity poses a complex scientific problem that translates into a challenging software engineering problem. Here I want to discuss "Cactus", a code that is developed and used at the Albert-Einstein-Institut (AEI, the Max-Planck-Institut für Gravitationsphysik), and several other institutions [75, 76, 77].

Referring to [75], the cactus code is a freely available modular portable and manageable environment for collaboratively developing high-performance multidimensional numerical simulations. Cactus provides a powerful application programming interface based on user modules (thorns) that plug into a compact core (flesh). Cactus is composed of modules that are independent of relativity, and of modules designed for relativity. The Cactus Computational Tool Kit supports a variety of supercomputing architectures and clusters, implements MPI-based parallelism for finite difference grids, several input/output layers, elliptic solvers, metacomputing, distributed computing, and visualization tools. Fixed and adaptive mesh refinement is under development. Cactus significantly enhances collaborative development by providing code sharing via CVS and defining appropriate interfaces for code combination. A large number of physics modules or thorns are available for numerical relativity and astrophysical applications, e.g. there are thorns for initial data, evolution routines, and data analysis. The first version of Cactus was created by J. Massó and P. Walker, and has been available for testing since April, 1997 [78]. The Cactus Computational Tool Kit (Cactus 4.0) saw its first public release as a community code in July, 1999. It is actively supported by a cactus maintenance team, and there is good documentation. Cactus is a "third generation" code, going back to the "G" [26] and "H" [28] codes. The key step taken forward is the massive investment in the collaborative infrastructure, which is now beginning to pay off. For many more details, see [75, 76].

So what does all of this mean? Suppose you want to run a black hole simulation. Cactus is not a high-level science tool where you get an executable with graphical user interface to input, say, the black hole masses and off it goes. Numerical relativity is still too experimental for that. At its heart, Cactus is a large collection of source files together with a sophisticated make system. The user decides what sources to include, then compiles the code. Runs are controlled by a text file containing parameters, e.g. for the grid size and the black hole masses. The sophistication lies in the ease with which code can be changed or added by single users without affecting functionality provided by others. Suppose a users wants to add a routine that computes the determinant of the metric. A new thorn is created with the source code, e.g. 20 lines of C or Fortran, and with files that inform Cactus about new parameters, new grid functions (say an array of reals with the name "detg"), and tell cactus when to call the new routine (in this case whenever analysis is done). This is work to be done by the thorn writer, but he or she gets the rest for free: set-up of a numerical grid, storage for g_{ab} and its determinant, evolution of g_{ab} according to, say, the ADM equations, parallel execution, input, output, adaptive mesh refinement, etc. When submitted to the Cactus code repository, any Cactus user can now make use of "detg".

Taking the viewpoint of a physicist, the Cactus infrastructure takes care of many computer tasks that often distract from science. To say that a simulation was carried out with Cactus can refer to Cactus, the Computational Tool Kit, in the same way that credit is given to MPI for parallelism, or Mathematica or Maple for symbolic computation. Cactus is successful if the science

outweighs the infrastructure. In order that Cactus does not remain a faceless collection of source code, I would like to give several science examples and also to mention at least a few names in connection with science projects. Work on hyperbolic methods in numerical relativity [79] was done by J. Massó, P. Walker, and others. A project on black hole excision techniques has been implemented as "Agave" by S. Brandt, M. Huq, P. Laguna, and others at Penn State University, which uses Cactus mainly for parallelism. Furthermore, the NASA Neutron Star Grand Challenge Project of W.-M. Suen, E. Seidel, and others, develops the so-called GR3D code [80], which is a version of Cactus for coupled spacetime and relativistic hydrodynamics evolution based on Riemann solvers. M. Miller implemented the key science module (MAHC) for GR3D, with further contributions from other members of the Grand Challenge [81, 82], see Sec. 7 for an application. Finally, Cactus is of course our platform for the binary black hole collisions reported on in Sec. 5 and the strong gravitational wave evolutions of Sec. 6. In this case, the code "BAM" originally developed in [31, 83, 41] contributed the multigrid elliptic solver for the initial data and for maximal slicing, and the Mathematica scripts of BAM were used to generate C code for the BSSN evolution. For analysis, an apparent horizon finder implemented by M. Alcubierre was used (there is also one available by C. Gundlach, [73]), and the wave extraction routines by G. Allen [35]. A much larger number of individuals than is apparent from the above citations has contributed to "the" Cactus code, see [75]. At this moment the Cactus 3.2 CVS repository lists 88 thorns, which range from private and under development to stable and public.

5   Grazing collision of black holes

The first crude but truly (3+1)-dimensional binary black hole simulation can be summarized as follows [41]. The approach taken was to address each of the items listed in the skeleton for evolution problems of black holes of Sec. 3.3 in the simplest possible manner that still allowed us to combine all the ingredients to a complete implementation. Initial data for two black holes, each with linear momentum and spin, is constructed using the puncture method [66] (see also [84]), in which the internal asymptotically flat regions of the holes are compactified so that the numerical domain becomes R^3. By construction the initial data is conformally flat. The evolution is performed with the original ADM equations and a leapfrog finite difference scheme. Maximal slicing and vanishing shift is chosen, i.e. physical singularities are avoided, while coordinate singularities typically do not occur for this elliptic slicing condition. At the outer boundary, the ADM variables are held constant, which works well for the achievable run times because a fixed mesh refinement of nested boxes (with finer resolution at the center) is used, and for large radii the lapse can approximate the Schwarzschild lapse for which Schwarzschild data would remain static. An important insight is that the puncture method, which can be made rigorous for initial data, can be numerically extended to the evolution equations so that no special inner boundary is present [41]. Analysis is restricted to apparent horizon

finding with a curvature flow method. These methods allow one to evolve for about $7M$, which is sufficient to observe the merger of the apparent horizons, but too short for wave extraction.

Currently, binary black hole mergers are simulated by our AEI/NCSA/-WashU/Palma collaboration, and in this section I summarize some of the preliminary results. These simulations build on [26, 40, 41] and introduce various improvements. On the technical side, for high-performance collaborative computing the code is implemented with Cactus 3.2. An improved apparent horizon finder is now available [73]. The comparatively slow maximal slicing can in many situations be replaced by "1+log" slicing (cmp. Sec. 3.2). No mesh refinement is used, but the outer boundary is treated with a radiative (Sommerfeld) boundary condition. The above plus the BSSN evolution system as given in [45] with a 3-step iterative Crank-Nicholson (ICN) scheme, allow run times of up to $30M$ for grazing collisions, compared to $7M$ for previous runs, and up to $50M$ for simpler data sets.

The important new result is that now for the first time the extraction of wave forms becomes possible with the methods tested in [35]. Let us discuss a concrete example. For initial data we choose the punctures of each hole on the y-axis at ±1.5, masses $m_1 = 1.5$ and $m_2 = 1$, linear momenta $P_{1,2} = (\pm2, 0, 0)$, and spins $S_1 = (-1/2, 1/2, 0)$ and $S_2 = (0, 1, 1)$ (all units normalized by $m_2 = 1$). The numerical grid has 385^3 points with grid spacing 0.2, which puts the outer boundary for a centered cube at a coordinate value of about 38. The initial ADM mass is $M = 3.11$, so the outer boundary is at about $12M$ (solving the constraints for the "bare" parameters increases the mass over the Brill-Lindquist vanishing spins and momenta value of $m_1 + m_2$). The total angular momentum is $J = 6.7$, which corresponds to an angular momentum parameter of $a/M = J/M^2 = 0.70$.

The black holes start out with separate marginally trapped surfaces forming the apparent horizon (although it may well be that they have a common event horizon). Fig. 2 shows the formation of a single marginally trapped surface surrounding the initial inner marginally trapped surfaces. The apparent horizon is defined by a type of minimal surface equation (e.g. [73]), and does not evolve continuously, rather a new "minimal" surface appears in a new location. The shading of the surfaces indicates the Gauss curvature on the surfaces. The area of the apparent horizon increases in these coordinates because grid points are falling into the black hole. In Fig. 3, two frames near the merger are shown together with isosurfaces of $\mathrm{Re}\psi_4$ as a wave indicator.

From the evolution, we can obtain an energy balance by comparing the energy carried by the various modes of the gravitational waves [35] with the difference in mass between the initial slice and the final black hole. For the latter, the apparent horizon mass is $M_{AH} = [(M_{ir})^2 + J^2/(2M_{ir})^2]^{1/2}$ with $(M_{ir})^2 = A_{AH}/(16\pi)$ and A_{AH} the numerically determined area of the apparent horizon of the final black hole. During the evolution, A_{AH} reaches a plateau, but then starts drifting upwards as the grid stretching becomes more severe.
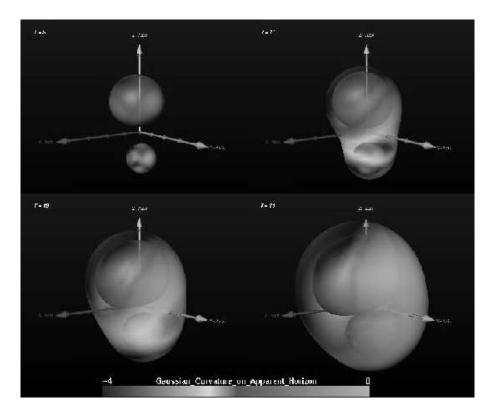
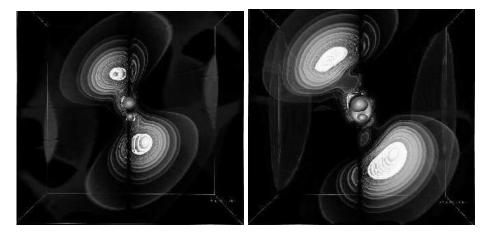Figure 2: The evolution of the apparent horizon during a grazing black hole collision ($t = 9$, 11, 16, 21).

Figure 3: Apparent horizon during a grazing black hole collision with Reψ_4 as a wave indicator.

With the plateau value for A_{AH} and $M_{ADM} \equiv M = 3.11$ we obtain

$$M_{ADM} - M_{AH} = 0.03 \approx 0.01 M_{ADM}. \tag{10}$$

A rough estimate for the radiated energy in all modes until $t = 30M$, with the extraction radius rather close to the system at $8M$, is

$$M_{RAD} = 0.007 - 0.008 M_{ADM}. \tag{11}$$

Even with all the current restrictions on accuracy coming from resolution, grid size, boundary treatment, and grid stretching, this energy balance can be considered to be a first physics result for such a grazing collision. We learn that for this data set roughly 1% of the total energy is emitted in gravitational waves. Clearly, a thorough parameter space study of such configurations is of interest. To make contact with astrophysical situations, more realistic initial data is probably needed (which ideally would be derived from the slow inspiral of the two black holes). A detailed report is in preparation.

6 Gravitational collapse of gravitational waves

One way to probe general relativity in the highly non-linear regime, which should also share some of the strong wave features of the grazing collision, is certainly through the gravitational collapse of gravitational waves to a black hole. As briefly mentioned in Sec. 2.1, one scenario is that of critical collapse [23]. One can construct a one-parameter family of initial data, and examine the region near the "critical" value for that parameter at which a black hole does or does not form. Not much is known in 3+1 dimensions [24], and the only study in axisymmetry is that of Abrahams and Evans [22, 25] for gravitational waves.

In this section I want to briefly discuss first results for non-axisymmetric collapse, cmp. [29]. We take as initial data a pure Brill type gravitational wave [85], later studied by Eppley [86, 87] and others [88]. The metric takes the form

$$ds^2 = \Psi^4 \left[e^{2q} \left(d\rho^2 + dz^2 \right) + \rho^2 d\phi^2 \right] = \Psi^4 \hat{ds}^2, \tag{12}$$

where q is a free function subject to certain boundary conditions. Following [35, 33, 89], we choose q of the form

$$q = a \, \rho^2 \, e^{-r^2} \left[1 + c \, \frac{\rho^2}{(1 + \rho^2)} \, \cos^2 (n\phi) \right], \tag{13}$$

where a, c are constants (a different from Sec. 5), $r^2 = \rho^2 + z^2$ and n is an integer. For $c = 0$, these data sets reduce to the Holz [88] axisymmetric form, recently studied in three-dimensional Cartesian coordinates in preparation for the present work [73]. Taking this form for q, we impose the condition of time-symmetry, and solve the Hamiltonian constraint numerically in Cartesian coordinates. An initial data set is thus characterized only by the parameters (a, c, n). For the case $(a, 0, 0)$, we found in [73] that no apparent horizon exists

in initial data for $a < 11.8$, and we also studied the appearance of an apparent horizon for other values of c and n.

For evolutions, we found that the BSSN system as given in [45] with maximal slicing, a 3-step ICN scheme, and a radiative boundary condition is sufficiently reliable even for the strong waves considered here. The key new extensions to previous BSSN results are that the stability can be extended to (i) strong, dynamical fields and (ii) maximal slicing, where the latter requires some care. Maximal slicing is defined by vanishing of the mean extrinsic curvature, $K=0$, and the BSSN formulation allowed us to cleanly implement this feature numerically, in contrast with the standard ADM equations.

As discussed in [29], axisymmetric data with $a = 4$ is subcritical, that is the imploding part of the wave disperses again, leaving flat space in a non-trivially distorted coordinate system. An amplitude of $a = 6$ gives a super-critical evolution as indicated by the formation of an apparent horizon. The "cartoon" method [90] to perform axisymmetric calculations in Cactus using three-dimensional Cartesian stencils on a two-dimensional slab allowed us to close in on the critical region near $a = 4.6$, but work on detection of critical phenomena is still in progress.

Fig. 4 shows the development of the data set (a=6, c=0.2, n=1), which has reflection symmetry across coordinate planes. The initial ADM mass of this data set turns out to be $M_{ADM} = 1.12$. Fig. 4a shows a comparison of the apparent horizons of this three-dimensional and the previous axisymmetric cases at t=10 on the x-z plane. The mass of the three-dimensional apparent horizon case is larger, weighing in at M_{AH}=0.99 (compared to $M_{AH}(2D) = 0.87$).

In Fig. 4b we show the $\{l=2, m=0\}$ wave form of this three-dimensional case, compared to the previous axisymmetric case. The $c = 0.2$ wave form has a longer wave length at late times, consistent with the fact that a larger mass black hole is formed in the three-dimensional case. Figs. 4c and 4d show the same comparison for the $\{l=4, m=0\}$ and $\{l=2, m=2\}$ modes respectively. Notice that while the first two modes are of similar amplitude for both runs, the three-dimensional $\{l=2, m=2\}$ mode is completely different; as a non-axisymmetric contribution, it is absent in the axisymmetric run (in fact, it does not quite vanish due to numerical error, but it remains of order 10^{-6}). We also show a fit to the corresponding quasi normal modes of a black hole of mass 1.0. The fit was performed in the time interval $(10, 36)$, and is noticeably worse if the fit is attempted to earlier times, showing that the lowest quasi normal modes dominate at around 10. The early parts of the wave forms $t < 10$ reflect the details of the initial data and BH formation process. This is especially clear in the $\{l=2, m=2\}$ mode, which seems to provide the most information about the initial data and the three-dimensional black hole formation process.

7   Minimal distortion shift

As a final example for recent advances in numerical relativity simulations, let me mention shift conditions in (3+1)-dimensional relativity. The first preliminary
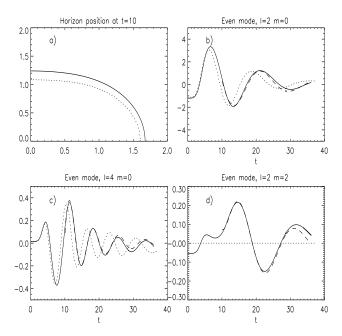
Figure 4: a) The solid (dotted) line is the apparent horizon for the 3D data set $(6, 0.2, 1)$ $((6, 0, 0))$ at $t=10$ on the x-z plane. b) The $\{l{=}2,m{=}0\}$ wave form for the 3D $(6, 0.2, 1)$ case at $r = 4$ (solid line) is compared to axisymmetric $(6, 0, 0)$ case (dotted line). The dashed line shows the fit of the 3D case to the corresponding mode for a black hole of mass 1.0. c) Same comparison for the $\{l{=}4,m{=}0\}$ wave form. d) Same comparison for the non-axisymmetric $\{l{=}2,m{=}2\}$ wave form.

16

test of a dynamically computed minimal distortion shift can be found in [30] for a Schwarzschild black hole on a 3+1 Cartesian grid, which is still the only example with black hole excision. Computational domains with holes pose a technical problem for the elliptic solver, which certainly will be solved (see for example [91]) once excision runs demand dynamic shifts.

A non-vanishing shift plays an important role in calculations that involve orbiting black holes or neutron stars, e.g. in post-newtonian calculations or Newtonian hydrodynamics for neutron stars. The freedom in the shift vector can in principle be used to obtain corotating coordinates or partially corotating coordinates (to counter frame dragging). A variational principle to minimize coordinate shear leads to the minimal distortion family of shift conditions, see [92]. Introducing again a conformal factor such that the conformal metric $\tilde{g}_{ab}$ has unit determinant, one can minimize

$$ S[\beta] = \int |\partial_t \tilde{g}|^2 dV = \int \tilde{g}^{ac} \tilde{g}^{bd} \partial_t \tilde{g}_{ab} \partial_t \tilde{g}_{cd} \sqrt{\det g} \, d^3 x, \tag{14} $$

which gives a vector elliptic equation for β^a,

$$ (\Delta_l \beta)^a = 2D_b(\alpha(K^{ab} - g^{ab}K/3)), \tag{15} $$

$$ (\Delta_l \beta)^a \equiv D_b D^b \beta^a + D_b D^a \beta^b - \frac{2}{3} D^a D_b \beta^b. \tag{16} $$

Note that if there exists a rotational Killing vector, minimal distortion can be trivially obtained [92], hence such shift conditions begin playing a non-trivial role only when one moves beyond axisymmetric simulations (see also [93, 94], and in particular [95] for spacetimes with approximate Killing vector fields).

There are now three examples for the application of dynamical shift conditions to binary neutron star simulations, which share the feature that with vanishing shift the code fails after far less than an orbit, while with minimal distortion shift for the first time fully relativistic simulations of one or more orbits become possible. In [96, 97], minimal distortion is approximated in a way that decouples the three equations but maintains key features. Preliminary experiments have also been performed for the NASA Neutron Star Grand Challenge using Cactus, the hydrodynamics module or "thorn" MAHC [81, 82], and the author's implementation of the vector Laplace operator (16) in BAM. The full minimal distortion equations are solved. One choice of initial data is that of irrotational neutron star binaries provided by the Meudon group ([98, 99], polytropic equation of state with $\gamma = 2$, $\kappa = 0.03c^2/\rho_{nuc}$, $M_1 = M_2 = 1.6M_{sol}$, $M/R = 0.14$, $d = 41km$). Fig. 5 shows four frames of an evolution project that was implemented and carried out this summer by M. Miller, N. Stergioulas, and M. Tobias. Without shift, the simulation crashes before less than 1/10th of an orbit is completed, with shift one observes about 3/4 of an orbit before the code fails when the two neutron stars merge. These first results can probably be improved significantly, but they already serve as a proof that non-vanishing shift is beneficial.
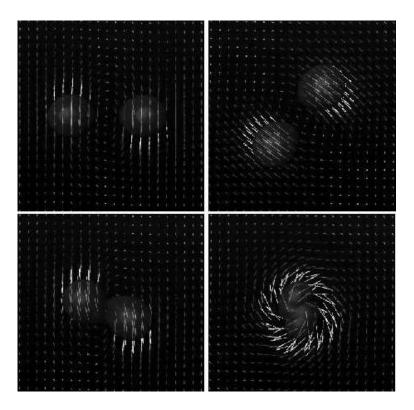
Figure 5: Binary neutron star orbit with minimal distortion shift. The neutron stars are represented by an isosurface at 1/10 of the central density, the shift vector by the arrows.

8   Conclusion

It is perhaps surprising how little has been achieved to date by numerical simulations of the Einstein equations for the two body problem. After all, the Einstein equations have been extensively studied for more than 80 years, and nowadays modern computational physics has successfully treated the partial differential equations of a large number of evolution problems. Why is it not possible to "simply solve" the problem with standard numerical methods on a big computer? To recall some of the issues raised above, (i) the Einstein equations do not lead to a unique or preferred set of 3+1 evolution equations, with an automatically stable numerical implementation, (ii) choosing lapse and shift is intricately coupled to the evolution, (iii) black holes pose a special challenge due to their singularities.

As a result, black hole simulations in numerical relativity still have to be called rather limited. Either special simplifications are introduced (axisymmetry, null coordinates adapted to single black holes), or the achieved numerical runtime is a limiting factor compared to the lowest quasi-normal ringing period of about $17M$. (3+1)-dimensional black hole evolutions with singularity avoiding slicing last to about $30M$ for simple data sets starting from time symmetry (vanishing extrinsic curvature) [26, 40]. The first evolution of truly three-dimensional binary black hole data (two black holes with spin and linear momentum) was performed in 1997 [41], crashing at $7M$, which allowed tracking the merging of apparent horizons but not wave extraction. Considering that the first 3+1 simulations of Schwarzschild were reported in 1995, one can certainly call the recent simulations of Sec. 5 with wave extraction and a run time of about $30M$ a significant step forward.

Several methods are under intense investigation that should allow us to evolve for hundreds of M or even longer. Here we mentioned black hole excision, improved evolution schemes, and shift conditions. Especially excision is expected to be essential. For the purpose of wave extraction, the schemes involving future null infinity are of particular interest. Furthermore, astrophysically more realistic initial data is needed as input for the above methods before we can make contact with gravitational wave astronomy.

How close is numerical relativity to the accurate prediction of gravitational wave forms for binary events [100]? The post-newtonian and the close-limit approximations are probably in good shape, but full numerical relativity will require two or more years to get ready. An introductory statement often heard during the last two decades is that one essential task of numerical relativity is to provide a catalog of wave forms which is essential for gravitational wave detection. This has changed. Numerical relativity will be essential in wave analysis, producing models for astrophysical scenarios that relate the wave forms to configuration parameters. For the detection as such, however, the task of producing a complete catalog appears to be too hard, and in particular, not a very sensible one. Note that matched filtering gives roughly a factor 5 in signal to noise for wave detection [101, 102]. Recently, the advantage of the perfect catalog over the best "blind" numerical methods has been reduced to a factor

of 2, e.g. [103]. This still corresponds to a factor of 100 in observable event rate, but on the other hand optimal matched filtering is assumed in this estimate. The emphasis in numerical relativity should therefore be shifted more towards producing reliable statements about global features of mergers as opposed to detailed wave forms. Predicting the duration of mergers, total energy emission, frequency range and frequency distribution of the signal will be more useful to methods as described in [101, 102, 103] and also more attainable in the near future. The black hole runs of Sec. 5 are being performed with this goal in mind.

References

[1] B. Schutz, gr-qc/9911034

[2] T. Damour, in *Relativistic Gravitation and Gravitational Radiation*, edited by J. Marck and J. Lasota (Cambridge University Press, Cambridge, England, 1997), p. 1

[3] L. Blanchet, in *Relativistic Gravitation and Gravitational Radiation*, edited by J. Marck and J. Lasota (Cambridge University Press, England, Cambridge, 1997), p. 33

[4] J. Pullin, in *Proceedings of GR15*, edited by N. Dadhich and J. Narlikar (Inter Univ. Centre for Astr. and Astrop., Puna, 1998), p. 87

[5] S. G. Hahn and R. W. Lindquist, Ann. Phys. **29** (1964) 304

[6] L. Smarr, Ph.D. thesis, University of Texas, Austin, Austin, Texas, 1975

[7] L. Smarr, Ann. N. Y. Acad. Sci. **302** (1977) 569

[8] K. Eppley, Ph.D. thesis, Princeton University, Princeton, New Jersey, 1975

[9] C. W. Misner, Ann. Phys. **24** (1963) 102

[10] J. York, in *Sources of Gravitational Radiation*, edited by L. Smarr (Cambridge University Press, Cambridge, England, 1979)

[11] S. L. Shapiro and S. A. Teukolsky, Phys. Rev. D **45** (1992) 2739

[12] P. Anninos *et al.*, Phys. Rev. Lett. **71** (1993) 2851

[13] P. Anninos *et al.*, Phys. Rev. D **52** (1995) 2044

[14] R. Matzner *et al.*, Science **270** (1995) 941

[15] P. Anninos and S. Brandt, Phys. Rev. Lett. **81** (1998) 508

[16] S. Brandt and P. Anninos, Phys. Rev. D **60** (1999) 084005

[17] S. Hughes *et al.*, Phys. Rev. D **49** (1994) 4004

[18] S. Brandt and E. Seidel, Phys. Rev. D **52** (1995) 870

20

[19] S. Brandt and J. A. Font, in *Proc. 8th M. Grossmann Meeting*, edited by T. Piran (World Scientific, Singapore, 1998), in press

[20] S. Brandt *et al.*, Phys. Rev. D, submitted, gr-qc/9807017

[21] S. L. Shapiro and S. A. Teukolsky, Phys. Rev. Lett. **66** (1991) 994

[22] A. Abrahams and C. Evans, Phys. Rev. D **46** (1992) R4117

[23] M. Choptuik, Phys. Rev. Lett. **70** (1993) 9

[24] C. Gundlach, Adv. Theor. Math. Phys **2** (1998) 1

[25] A. Abrahams and C. Evans, Phys. Rev. Lett. **70** (1993) 2980

[26] P. Anninos *et al.*, Phys. Rev. D **52** (1995) 2059

[27] M. Shibata and T. Nakamura, Phys. Rev. D **52** (1995) 5428

[28] P. Anninos *et al.*, Phys. Rev. D **56** (1997) 842

[29] M. Alcubierre *et al.*, gr-qc/9904013

[30] G. E. Daues, Ph.D. thesis, Washington University, St. Louis, Missouri, 1996

[31] B. Brügmann, Phys. Rev. D **54** (1996) 7361

[32] C. Bona, J. Massó, E. Seidel, and P. Walker, gr-qc/9804065, submitted to Phys. Rev. D

[33] K. Camarda, Ph.D. thesis, University of Illinois at Urbana-Champaign, Urbana, Illinois, 1998

[34] K. Camarda and E. Seidel, Phys. Rev. D **59** (1999) 064026

[35] G. Allen, K. Camarda, and E. Seidel, gr-qc/9806036, submitted to Phys. Rev. D

[36] G. B. Cook *et al.*, Phys. Rev. Lett **80** (1998) 2512

[37] R. Gomez, R. Marsa, and J. Winicour, Phys. Rev. D **56** (1997) 6310

[38] R. Gomez, L. Lehner, R. Marsa, and J. Winicour, Phys. Rev. D **57** (1998) 4778

[39] R. Gomez *et al.*, Phys. Rev. Lett. **80** (1998) 3915

[40] P. Anninos, J. Massó, E. Seidel, and W.-M. Suen, Physics World **9** (1996) 43

[41] B. Brügmann, Int. J. Mod. Phys. D **8** (1999) 85

[42] R. Arnowitt, S. Deser, and C. W. Misner, in *Gravitation: An Introduction to Current Research*, edited by L. Witten (John Wiley, New York, 1962), pp. 227–265

[43] H. Friedrich, Class. Quant. Grav. **13** (1996) 1451

[44] O. Reula, Living Reviews in Relativity **1** (1998)

[45] T. W. Baumgarte and S. L. Shapiro, Physical Review D **59** (1999) 024007

[46] A. Arbona, C. Bona, J. Massó, and J. Stela, gr-qc/9902053

[47] M. Alcubierre, B. Brügmann, M. Miller, and W.-M. Suen, Phys. Rev. **D60** (1999) 064017

[48] S. Frittelli and O. Reula, gr-qc/9904048

[49] M. Alcubierre *et al.*, gr-qc/9908079

[50] T. W. Baumgarte, S. A. Hughes, and S. L. Shapiro, gr-qc/9902024

[51] T. W. Baumgarte *et al.*, gr-qc/9907098

[52] M. Alcubierre *et al.*, in preparation (1999)

[53] I. Novikov, Ph.D. thesis, Shternberg Astronomical Institute, Moscow, 1962

[54] C. W. Misner, K. S. Thorne, and J. A. Wheeler, *Gravitation* (W. H. Freeman, San Francisco, 1973)

[55] J. Thornburg, Classical and Quantum Gravity **4** (1987) 1119

[56] E. Seidel and W.-M. Suen, Phys. Rev. Lett. **69** (1992) 1845

[57] H. Friedrich, Proc. Roy. Soc. London **A 375** (1981) 169

[58] H. Friedrich, Proc. Roy. Soc. London **A 378** (1981) 401

[59] P. Hübner, gr-qc/9804065

[60] J. Frauendiener, gr-qc/9808072

[61] R. Isaacson, J. Welling, and J. Winicour, J. Math. Phys. **24** (1983) 1824

[62] N. Bishop, C. Clarke, and R. d'Inverno, Class. Quant. Grav. **7** (1990) L23

[63] J. Winicour, Living Reviews in Relativity **1** (1998)

[64] J. Winicour, in *Yukawa Meeting 1999*, gr-qc/9911106

[65] G. B. Cook *et al.*, Phys. Rev. D **47** (1993) 1471

[66] S. Brandt and B. Brügmann, Phys. Rev. Lett. **78** (1997) 3606

[67] A. Lichnerowicz, J. Math Pures et Appl. **23** (1944) 37

[68] Y. Choquet-Bruhat, in *Gravitation: An Introduction to Current Research*, edited by L. Witten (John Wiley, New York, 1962)

[69] M. Alcubierre, Phys. Rev. D **55** (1997) 5981

[70] M. Alcubierre and J. Massó, Phys. Rev. D Rapid Comm. **57** (1998) 4511

[71] A. M. Abrahams *et al.*, Physical Review Letters **80** (1998) 1812

[72] J. Frauendiener, Phys. Rev. D **58** (1998) 064002

[73] M. Alcubierre *et al.*, gr-qc/9809004

[74] A. Abrahams and C. Evans, Phys. Rev. D **37** (1988) 318

[75] *http://www.cactuscode.org*

[76] E. Seidel and W.-M. Suen, J. Comp. Appl. Math. (1999), in press

[77] G. Allen, T. Goodale, and E. Seidel, in *7th Symposium on the Frontiers of Massively Parallel Computation-Frontiers 99* (IEEE, New York, 1999)

[78] J. Massó and P. Walker, (1998), in preparation

[79] C. Bona, J. Massó, E. Seidel, and P. Walker, gr-qc/9804065, submitted to Phys. Rev. D

[80] For the NASA Neutron Star Grand Challenge Project, see, e.g., http://wugrav.wustl.edu/Relativ/nsgc.html.

[81] J. A. Font, M. Miller, W. M. Suen, and M. Tobias, gr-qc/9811015, submitted to Phys. Rev. D

[82] M. Miller, W.-M. Suen, and M. Tobias, gr-qc/9904041

[83] B. Brügmann, in *Proceedings of The 18th Texas Symposium on Relativistic Astrophysics*, edited by J. F. A. Olinto and D. Schramm (World Scientific, Singapore, 1998)

[84] R. Beig and N. O'Murchadha, Class. Quant. Grav. **13** (1996) 739

[85] D. S. Brill, Ann. Phys. **7** (1959) 466

[86] K. Eppley, Phys. Rev. D **16** (1977) 1609

[87] K. Eppley, in *Sources of Gravitational Radiation*, edited by L. Smarr (Cambridge University Press, Cambridge, England, 1979), p. 275

[88] D. Holz, W. Miller, M. Wakano, and J. Wheeler, in *Directions in General Relativity: Proceedings of the 1993 International Symposium, Maryland; Papers in honor of Dieter Brill*, edited by B. Hu and T. Jacobson (Cambridge University Press, Cambridge, England, 1993)

[89] S. Brandt, K. Camarda, and E. Seidel, in *Proc. 8th M. Grossmann Meeting*, edited by T. Piran (World Scientific, Singapore, 1998), in press

[90] M. Alcubierre *et al.*, gr-qc/9908012

[91] P. Diener, N. Jansen, A. Khokhlov, and I. Novikov, gr-qc/9905079

[92] L. Smarr and J. York, Phys. Rev. D **17** (1978) 2529

[93] R. Beig and P. Chrusciel, Class. Quant. Grav. **14** (1997) A83

[94] D. Garfinkle and C. Gundlach, Class. Quant. Grav., gr-qc/9908016, to be published

[95] P. R. Brady, J. D. E. Creighton, and K. S. Thorne, gr-qc/9804057

[96] T. Nakamura and K. ichi Oohara, gr-qc/9812054

[97] M. Shibata, Prog. Theor. Phys. **101** (1999) 1199

[98] S. Bonazzola, E. Gourgoulhon, and J.-A. Marck, Phys.Rev.Lett. **82** (1999) 892

[99] S. Bonazzola, E. Gourgoulhon, and J.-A. Marck, Proceedings of the 19th Texas Symposium (1998), gr-qc/9904040

[100] This review is based on a talk given at the Journées Relativistes 1999, which were held at Weimar. With 1999 the Year of Goethe, and Weimar being the town of Goethe, I simply have to classify the final question as a "Gretchenfrage". This is a special type of question aimed at something fundamental. The illiterate but morally superior Gretchen asks worldly Dr. Faust how he stands on religion. Faust first tries to dodge the question with witty remarks, then upon Gretchen's insistence launches into a complicated confession which probably leaves the audience more confused than convinced. Of course, scientific review articles are much more to the point when addressing fundamental questions.

[101] Éanna É. Flanagan and S. A. Hughes, Phys. Rev. D **57** (1998) 4535

[102] Éanna É. Flanagan and S. A. Hughes, Phys. Rev. D **57** (1998) 4566

[103] W. Anderson and R. Balasubramanian, Phys. Rev. D **60** (1999) 102001

[104] For recent visualizations of Cactus runs see the movies page at http://jean-luc.aei-potsdam.mpg.de